Journal of
Composites Science

MDPI

Article

Polymerization Shrinkage, Hygroscopic Expansion, Elastic Modulus and Degree of Conversion of Different Composites for Dental Application

Alexandre Luiz Souto Borges [1], Amanda Maria de Oliveira Dal Piva [2], Sabrina Elise Moecke [1], Raquel Coutinho de Morais [1] and João Paulo Mendes Tribst [2,*]

[1] Institute of Science and Technology, São Paulo State University (Unesp), São José dos Campos 12245-000, Brazil; alexanborges@gmail.com (A.L.S.B.); sabrina.moecke@unesp.br (S.E.M.); raquel.coutinho@unesp.br (R.C.d.M.)
[2] Academic Centre for Dentistry Amsterdam (ACTA), University of Amsterdam and Vrije Universiteit Amsterdam, 1081 LA Amsterdam, The Netherlands; amodalpiva@gmail.com
* Correspondence: joao.tribst@gmail.com

Abstract: Objectives: To characterize the mechanical properties of different resin-composites for dental application. Methods: Thirteen universal dentin shade composites (n = 10) from different manufacturers were evaluated (4 Seasons, Grandio, Venus, Amelogen Plus, P90, Z350, Esthet-X, Amaris, Vita-l-escence, Natural-Look, Charisma, Z250 and Opallis). The polymerization shrinkage percentage was calculated using a video-image recording device (ACUVOL—Bisco Dental) and the hygroscopic expansion was measured after thermocycling aging in the same equipment. Equal volumes of material were used and, after 5 min of relaxation, baseline measurements were calculated with 18 J of energy delivered from the light-curing unit. Specimens were stored in a dry-dark environment for 24 h then thermocycled in distilled water (5–55 °C for 20,000 cycles) with volume measurement at each 5000 cycles. In addition, the pulse-excitatory method was applied to calculate the elastic modulus and Poisson ratio for each resin material and the degree of conversion was evaluated using Fourier transform infrared spectroscopy. Results: The ANOVA showed that all composite volumes were influenced by the number of cycles (α = 0.05). Volumes at 5 min post-polymerization (12.47 ± 0.08 cm^3) were significantly lower than those at baseline (12.80 ± 0.09 cm^3). With regard to the impact of aging, all resin materials showed a statistically significant increase in volume after 5000 cycles (13.04 ± 0.22 cm^3). There was no statistical difference between volumes measured at the other cycle steps. The elastic modulus ranged from 22.15 to 10.06 GPa and the Poisson ratio from 0.54 to 0.22 with a significant difference between the evaluated materials (α = 0.05). The degree of conversion was higher than 60% for all evaluated resin composites.

Keywords: composite dental resin; dental materials; polymerization; video recording

Citation: Borges, A.L.S.; Dal Piva, A.M.d.O.; Moecke, S.E.; de Morais, R.C.; Tribst, J.P.M. Polymerization Shrinkage, Hygroscopic Expansion, Elastic Modulus and Degree of Conversion of Different Composites for Dental Application. *J. Compos. Sci.* **2021**, *5*, 322. https://doi.org/10.3390/jcs5120322

Academic Editor: Masao Irie

Received: 22 November 2021
Accepted: 7 December 2021
Published: 10 December 2021

1. Introduction

In recent years, there has been an increasing interest in the development of new dental adhesives and composites for direct restorations. The main challenge of developing these materials is to provide an effective bond strength to the hard tissues, such as enamel and dentin, as well as lower or no polymerization shrinkage [1,2]. In addition, the mechanical and chemical properties of these materials have been improved along the years [1–4], positively affecting their clinical performance. The aesthetic restorative technique has also been improved, which increases the longevity of the resin-based restorations, especially for posterior teeth [4–6]. The maintenance of the marginal sealing and good quality of restoration filling techniques are the main focus during the treatment with conservative (non-replacement) dental restorations [7,8]. However, the incidence of marginal gaps can range from 1.67% to 5.68% of the total volume of the restoration [9], and can be

fulfilled by oral fluids, which contain bacteria responsible for the post-sensitivity and for caries lesions around restorations [10–12], compromising the clinical success. Complex interactions in adhesive interfaces such the underperformed bonding approach associated with high polymerization shrinkage strain, stress, and elastic modulus [13–16], rather than the differences in the composite formulation, can also lead to interfacial gaps, affecting the restoration integrity [17]. However, some authors reported that nanocomposites might lead to less gap formation at the resin–dentin interface [14].

When the composites initiate the polymerization process, stress is generated as a result of shrinkage. This phenomenon is a leading reason for bond failures in adhesive restorations. The stress is influenced by the restorative technique, mechanical properties, polymerization rate [18,19], and for some C-Factors, in particular small cavities [20]. As a measure of a restoration's confinement, the C-factor (Fc) is defined as the ratio of the bonded to not-bonded (free) surfaces of the restoration [21]. It is hypothesized that shrinkage stress increases with an increasing C-factor [21,22]. The constraints and stress magnitude generated in dental restorations are highly non-uniform, therefore not only the C-factor should be considered when evaluating the stress state [23]. The volumetric shrinkage is observed at both pre-gel and post-gel phases. The polymerization shrinkage starts immediately after the light activation, however at the post-gel phase it is possible to achieve an increase in hardness, reflecting the increase of elastic modulus of the resinous material, which is capable of creep. If the viscosity is already high, the stress developed by the polymerization shrinkage is not compensated anymore, affecting the interfacial bonding [23,24].

There are many testing systems for measuring the shrinkage stress and strain of resin-based materials, showing few similarities for the commercial composites [25]. Some authors used [26] the mercury dilatometer method and identified that the molecular weight and the molecular structure configuration of different monomers can affect the shrinkage. Another method is to measure the dimensional alterations in composites during the polymerization, using electrical strain gauges bonded to the composite specimens [27]. Previous authors found that the linear shrinkage reduced with the increase of the thickness of the specimen and with the distance of the light source tip to the resin surface [28]. When a material presents a low volumetric shrinkage, it does not mean that low shrinkage stresses will be generated after polymerization and for this reason the investigation of the elastic modulus is fundamental for the understanding of the stress generation [29,30].

Some authors have also found that not all low-shrinkage composites demonstrated reduced polymerization shrinkage and mentioned that a low post-gel shrinkage must be associated to a relatively low elastic modulus, in order to reduce the polymerization stress [3]. Although there are several methods for measuring the polymerization shrinkage, each of them presents advantages and disadvantages. The mercury capilar dilatometer is an efficient example to obtain shrinkage data, however it is too complex and limited to measure chemical composites, as it has to be prepared before its placement into the dilatometer [31]. Some authors calculated the volumetric shrinkage by the linear contraction, assuming that the composite material has an isotropic behavior [32], however this is not what happens for all cases. Therefore, the development of studies that characterize different properties from the available dental biomaterials could provide suitable data to better predict the clinical behavior of dental restorations. The aim of this study was to evaluate the polymerization shrinkage, the hygroscopic expansion during aging, elastic modulus, Poisson ratio, and degree of conversion of thirteen composites.

2. Materials and Methods

All materials used in this study are represented in Table 1. The chemical formula for the monomers presented in Table 1 are summarized in Figure 1. Polymerization shrinkage and hygroscopic expansion by water sorption were performed and described as follows.

Table 1. Materials used in this study.

Materials (Batch)	Manufacturer	Mean Filler Size (μm)	% Filler (Weight)	% Filler (Volume)	Filler Type	Organic Matrix	Manufacture's Classification
Venus (#010313)	Heraeus Kulzer, GMbH & Co, Kg, Germany	0.01–0.07	78%	61%	SiO_2, Barium, aluminiumfluoride	BisGMA. TEGDMA	Nanohybrid
Charisma (#010401)		0.002–0.7	78%	61%	Fluoride, barium, SiO_2	BisGMA, TEGDMA	Hybrid
Filtek Supreme (#FBU)	3M ESPE, St. Paul, MN, USA	0.005–0.02/0.6–1.4	78.5%	59.5%	SiO_2	BisGMA, BisEMA, UDMA, TEGDMA	Nanohybrid
Filtek P 90 (#N183458)		0.04–1.7	77%	51%	Quartz, fluoride, Itria fluoride	Siloranes	Nanohybrid
Filtek Z250 (#7EE)		0.01–3.5	78%	60%	SiO_2	BisGMA, UDMA, BisEMA	Hybrid
4 Seasons (#N48095)	Ivoclar Vivadent, São Paulo, SP, Brazil	0.6	76%	58%	Barium, Aluminium fluorsilicate, SiO_2	BisGMA, TEGMA, UDMA	Hybrid
Opallis (#210619)	FGM, Joinville, SC, Brazil	0.5	79 %	58%	Barium, aluminiumsilicate	BisGMA, BisEMA, TEGDMA	Hybrid
EsthetX (#100522)	Dentsply Detrey GmbH, Konstanz, Germany	<1.0	86%	60%	Barium fluoralumínium, borosilicate, SiO_2	UDMA, BisGMA, TEGDMA	Hybrid
Natural Look (#09080800)	DFL, Rio de Janeiro, RJ, Brazil	0.5	77%	59%	Barium amorphous silicate	BisGMA, BisEMA, TEGDMA	Hybrid
Amaris (#1024125)	VOCO, GMBH, Germany	0.7	80 %	64%	Silanized ceramic particles SiO_2	BisGMA, TEGDMA	Hybrid
Grandio (#1031020)		0.7	80%	63%	Silanized ceramic particles SiO_2	BisGMA, TEGDMA	Hybrid
Vit-l-escence (#B5L7Y)	Ultradent Products USA	0.7	75%	52%	Silanized ceramic particles SiO_2	BisGMA	Microhybrid
Amelogem PLUS (#B5M99)		0.7	76%	61%	SiO_2	BisGMA, TEGDMA	Hybrid

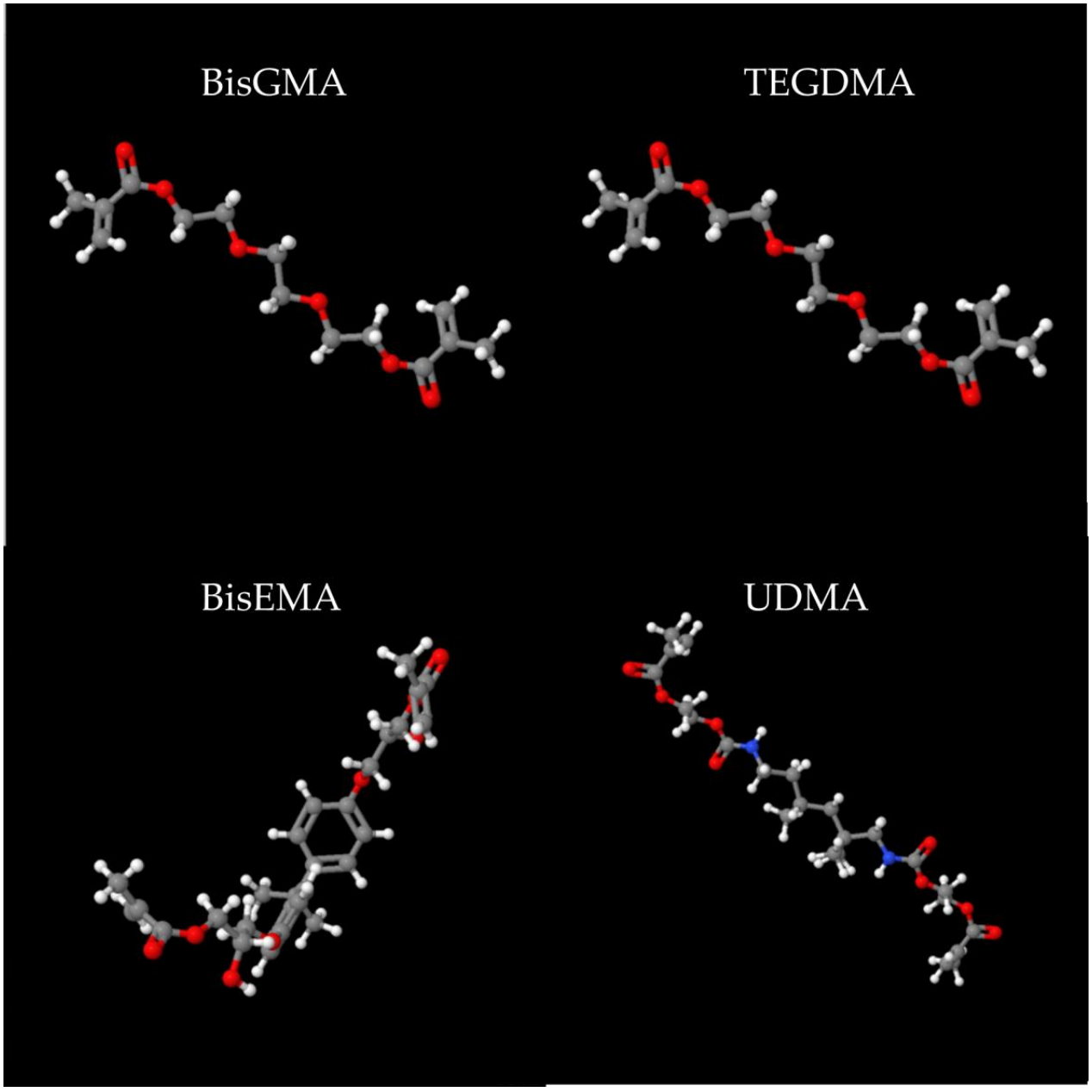

Figure 1. Molecular 3D structure of monomers commonly applied in dental composites. Note: Reprinted from ChemSpider, search and share chemistry.

2.1. Polymerization Shrinkage Measurement

Accurate volumetric shrinkage was measured using the video-imaging device (AcuvolTM, Bisco Inc., Schaumburg, IL, USA). This apparatus processes the images generated and performs the volume analysis simultaneously to the light-curing [33]. The accuracy of this instrument is 0.1% of volumetric alteration, considering specimens of approximately 15 µL [34]. To measure the polymerization shrinkage, a small portion of the composite was manually shaped in a polytetrafluoroethylene die, 4.8 mm in diameter at its base and 1.3 mm in height, resulting in a spherical cap shape (Figure 2).

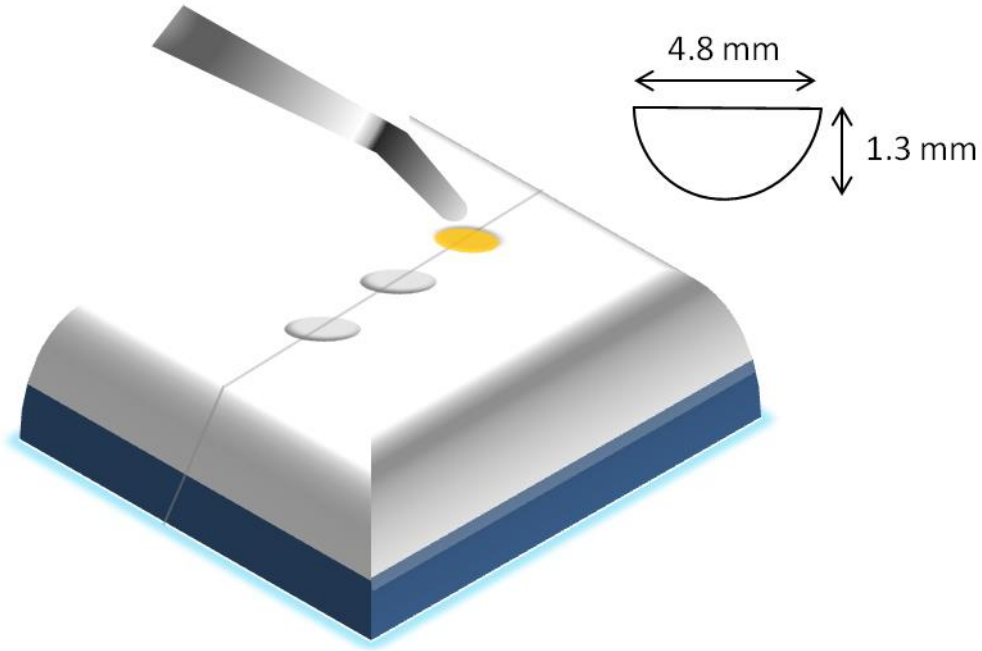

Figure 2. Scheme of polytetrafluoroethylene die used in the present study. The shape allowed the dental resin composite placement with standardized volume.

This set-up was then placed in a support in front of the load device coupled to the recording camera of the equipment (Figure 3). All specimens were stored for 5 min before the first volume measurement in an attempt to eliminate the influence of the relaxation generated by the gravity [33,34].

Figure 3. Light-curing of the specimen in position.

The total theoretical volume of the composite was 12.91 mm^3 and it was calculated by the formula of the spherical cap volume:

$$V = \frac{1}{6\pi h\ (3a^2) + h^2)}$$

where h is the height (1.3 mm) and a (2.4 mm) is the radius of the spherical cap base.

The area subjected to the light irradiation was calculated by the formula of the superficial area of the spherical cap as follows:

$$A = 2\pi rh$$

where r is the radius of the spherical cap base.

After the second measurement, the material was light-cured for 40 s using an LED unit (KaVo Poly Wireless, KaVo, São Paulo, Brazil). The light curing unit tip (Ø = 8.2 mm) was placed 1 mm from the top of the composite specimen. Before the test, the irradiation was checked using a radiometer (Radiômetro LED, Kordortech, São Carlos, Brazil). This procedure was repeated before the polymerization of each specimen to ensure that the same amount of energy (18 J) was delivered to all samples.

The volumetric shrinkage was recorded 5 min after the light activation, in an attempt to balance the specimens' temperature with the room temperature. A second measurement was then made and the subtraction of the first reading of the volume showed the volumetric shrinkage of the composite (Figure 3).

Ten specimens were obtained from each composite (n = 10) (Table 1). To determine the sample size, the normality of the pilot study data was verified by the Kolmogorov–Smirnov test ($p > 0.05$). Using the OpenEpi website, a power of 95.4% was calculated using a two-sided 95% confidence interval for 8 samples per group. However, 10 samples were selected to increase the safety factor. The standard deviation of the volumes obtained was maintained lower than 10%. To avoid light overexposure, the environment of the test was prepared with the use of an orange filter over the equipment in a dark room. Data were subjected to two-way ANOVA and Tukey tests, $p < 0.05$.

2.2. Hygroscopic Expansion

After the volumetric shrinkage test, the specimens were maintained in a dried condition at 37 °C for 24 h in a dark room. The humidity was controlled by the use of a dark chamber with silica gel to store the samples. Then, they were subjected to a new volume recording for analyzing the influence of the water sorption on the total specimen volume.

A sequence of 5000, 10,000, 15,000, and 20,000 aging cycles in distilled water was performed at 5 °C and 55 °C, and at the end of each cycle step the specimens were dried with a soft air jet for 15 s and repositioned at the equipment for new measurements. Data was subjected to two-way ANOVA and Tukey tests, $p < 0.05$.

2.3. Elastic Modulus and Poisson Ratio

Elastic modulus and Poisson ratio were measured by the non-destructive Impulse Excitation Technique (n = 8) using the equipment Sonelastic® (ATCP Physical Engineering, Ribeirão Preto, Brazil) using bar shaped specimens (20 × 10 × 4 mm). The impulse excitation technique (ASTM E1876) consists in determining the elastic modulus of the resin material based on the natural frequency of a regular geometry sample (in this study bar-shaped samples) [35]. The frequencies were excited by a short mechanical impulse, followed by the acquisition of the acoustic response using a high-sensitive microphone. After that, the software determines by means of a numerical calculation from the acoustic signal that was captured in order to obtain the frequency spectrum (fast Fourier transform). Based on this, the dynamic elastic modulus was determined using the ASTM standard, which considers the specimen geometry, mass, dimensions, and frequencies obtained using the equipment [35,36]. The characterization of the Poisson ratio using impulse excitation

technique occurred indirectly. It was obtained by correlating the Elastic modulus and the shear modulus of each material. The equations come from the elasticity theory and are directly related to the stiffness matrices involving the symmetry present in the sample [35]. They are shown below:

$$v = \frac{E}{2G} - 1$$

where E is the Elastic modulus; G, the shear modulus; v, the Poisson ratio of an isotropic material. Data were subjected to statistical analysis using one-way ANOVA and Tukey tests, $p < 0.05$.

2.4. Degree of Conversion

For each composite material, disc-shaped specimens (diameter: 5 mm; thickness: 4 mm) (N = 30) were prepared [37]. The polishing was performed 24 h after the sample polymerization, until the complete cure of the resinous materials. In order to remove the oxygen-inhibited layer, each sample was finished with wet silicone carbide papers 600-grit up to 1200-grit and polished (Strues, Model DP 10, Panambra Ind. & Tec. S.A., São Paulo, Brazil) with diamond paste (3 μm). The surfaces were analyzed by FT-Raman spectroscopy in order to evaluate the degree of conversion. The spectra of the uncured and cured resins were obtained by an FT-Raman Spectrometer (RFS 100/S, BrukerInc, Karlsruhe, Germany) using 100 scans. The spectrum resolution was set at 4 cm^{-1}. The specimens were excited by the defocused line of an Nd:YAG laser source at λ = 1064.1 nm with maximum laser power of approximately 90 mW at the specimen. The uncured resin was positioned on an aluminum rod in a sample holder mounted on an optical rail for spectrum collection [35]. For the cured specimens, three spectra of the top surface and another three spectra of the bottom surface were collected, resulting in a total of 480 spectra. Based on the measurements, one average spectrum for each surface was obtained, resulting in 160 spectra. The average FT-Raman spectra were analyzed by selecting a range between 1590 and 1660 cm^{-1}. The Raman peaks corresponding to the vibrational stretching modes at 1610 and 1640 cm^{-1} were fitted in Gaussian shapes to obtain the height of the peaks using specific software (Microcal Software Inc., Northampton, MA, USA). A comparison of the height ratio of the aliphatic carbon–carbon double bond (C=C) at 1640 cm^{-1} with that of the aromatic component at 1610 cm^{-1} for the cured and uncured conditions was performed in order to estimate the DC using Equation (1). The aromatic C=C peak at 1610 cm^{-1} originated from the aromatic bonds of the benzene rings in the monomer molecules, and its intensity remains unchanged during the polymerization reaction [37]. The mean value and standard deviation of the DC were calculated for each series, where R is the percentage of uncured resin that is determined by a band height at 1640 cm^{-1}/band height at 1610 cm^{-1}.

$$R_U = \frac{\text{Band height at 1640 cm}^{-1}}{\text{Band height at 1610 cm}^{-1}} \quad (1)$$

$$R_P = \frac{\text{Band height at 1614 cm}^{-1}}{\text{Band height at 1640 cm}^{-1}} \quad (2)$$

$$DC\ (\%) = 11 \times [1 - (R_P / R_U)] \quad (3)$$

where: R_U is the unpolymerized resin; R_P is the polymerized resin. Data were subjected to one-way ANOVA and Tukey tests, $p < 0.05$.

3. Results

Data were grouped for the first two measurements where the polymerization shrinkage occurs immediately and after 24 h (Figure 4).

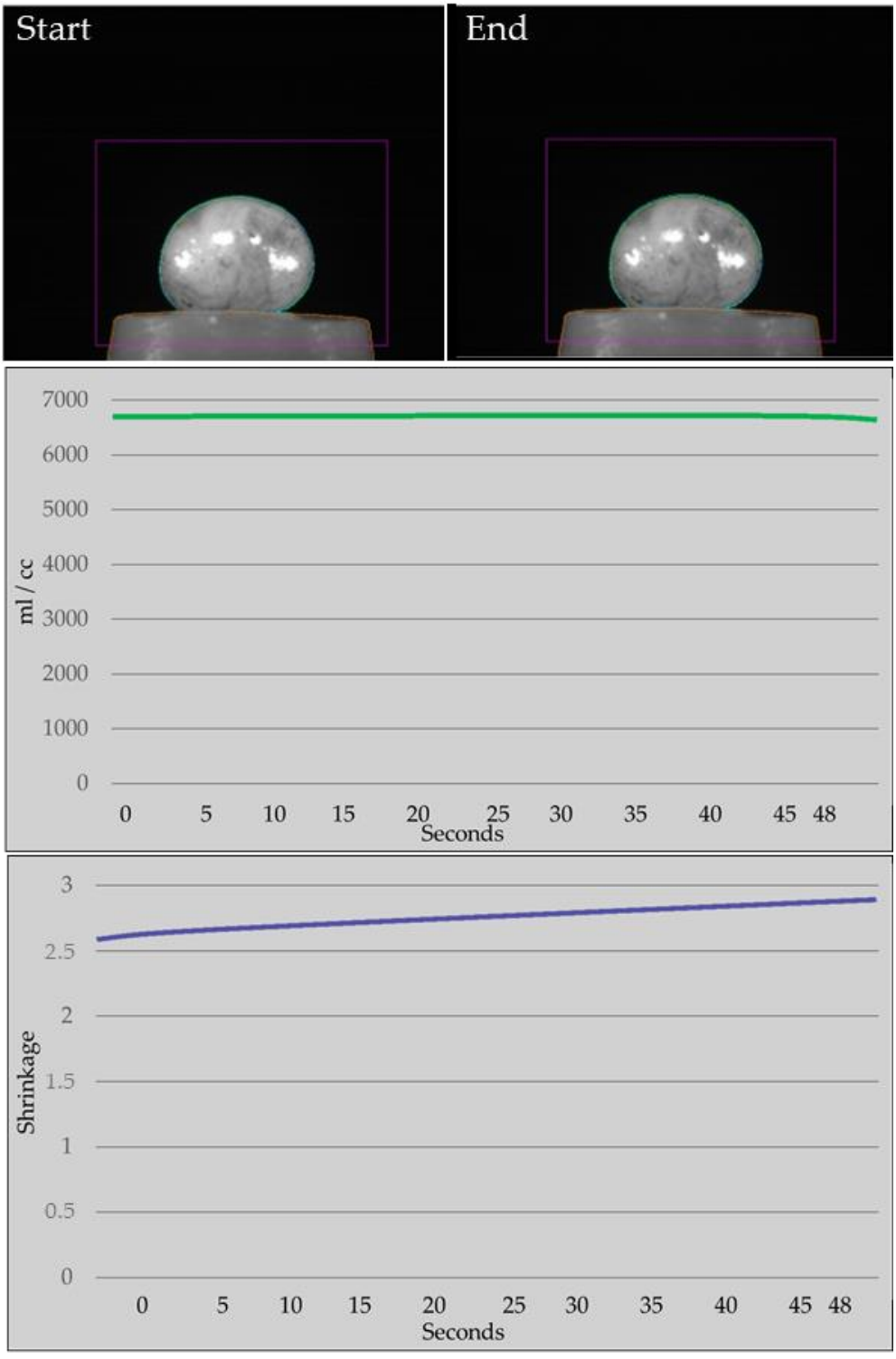

Figure 4. Analysis of images before and after polymerization. The graphs show the shrinkage by time.

After normality check, the two-way ANOVA was performed considering Material and Time as factors for the evaluation of the volumetric shrinkage data. The ANOVA test showed F-values for Material, Time, and interaction of, respectively 53.85, 140.17, and 5.8, and for all, p-value < 0.001 (Supplementary material: Table S1). There is a significant difference between materials (Table 2). In addition, all composites' volumetric shrinkages

were influenced by the post-polymerization time (24 h with 3.11% and 5 min with 2.49%). The interaction between both factors was also significant (Table 3).

Table 2. Mean and standard deviation for the volumetric shrinkage according to the factor resin composite materials. Same Capital Letter(s) means no statistical difference among groups ($\alpha = 0.05$).

Material	Mean ± Stand. Dev.	Grouping							
Vit-L-Escence	3.83 ± 0.51	A							
Natural look	3.52 ± 0.58	A	B						
Venus	3.21 ± 0.16		B	C					
4 Seasons	3.18 ± 1.04		B	C	D				
Opallis	3.15 ± 0.28		B	C	D	E			
Amelogen	2.97 ± 0.18			C	D	E			
EsthetX	2.89 ± 0.33			C	D	E	F		
Z350	2.75 ± 0.64				D	E	F		
Charisma	2.71 ± 0.20					E	F		
Amaris	2.51 ± 0.70						F	G	
Z250	2.48 ± 0.68						F	G	
Grandio	2.18 ± 0.70							G	
P90	1.04 ± 0.41								H

Table 3. Mean and standard deviation for the volumetric shrinkage according to the interaction of both factors, resin composite materials and time. Same Capital Letter(s) means no statistical difference among groups ($\alpha = 0.05$).

Material × Time	Mean ± Stand. Dev.	Grouping									
Vit-L-Escence × 24 h	4.31 ± 0.14	A									
4 Seasons × 24 h	3.93 ± 1.03	A	B								
Natural look × 24 h	3.87 ± 0.64	A	B	C							
Vit-L-Escence × 5 min	3.34 ± 0.17		B	C	D						
Venus × 24 h	3.30 ± 0.17		B	C	D						
Z350 × 24 h	3.26 ± 0.51		B	C	D	E					
Opallis × 24 h	3.22 ± 0.38			C	D	E	F				
EsthetX × 24 h	3.18 ± 0.20			C	D	E	F				
Natural look × 5 min	3.17 ± 0.14				D	E	F				
Venus × 5 min	3.13 ± 0.09				D	E	F	G			
Opallis × 5 min	3.08 ± 0.11				D	E	F	G			
Amelogen × 5 min	3.00 ± 0.14				D	E	F	G			
Amelogen × 24 h	2.93 ± 0.22				D	E	F	G	H		
Charisma × 24 h	2.90 ± 0.09				D	E	F	G	H		
Amaris × 24 h	2.88 ± 0.84				D	E	F	G	H		
Z250 × 24 h	2.87 ± 0.90				D	E	F	G	H		
Grandio × 24 h	2.68 ± 0.69				D	E	F	G	H	I	
EsthetX × 5 min	2.59 ± 0.06					E	F	G	H	I	
Charisma × 5 min	2.53 ± 0.09						F	G	H	I	
4 Seasons × 5 min	2.43 ± 0.07							G	H	I	
Z350 × 5 min	2.24 ± 0.16								H	I	J
Amaris × 5 min	2.13 ± 0.07									I	J
Z250 × 5 min	2.08 ± 0.05									I	J
Grandio × 5 min	1.68 ± 0.07										J
P90 × 24 h	1.09 ± 0.14										K
P90 × 5 min	0.98 ± 0.08										K

After normality check, the two-way ANOVA was performed considering Material and Time as factors for the evaluation of the hygroscopic expansion (caused by the water sorption) data. The ANOVA showed F-values and *p*-value for Material, Time, and interaction of, respectively, 1.47 and 0.131; 19.32 and $p < 0.001$; and, 1.09 and 0.294 (Supplementary material: Table S2). There is no significant difference between the materials. However, the period of evaluation was significant between the groups. There was no significant interaction between the factors. Table 4 summarizes the average data distribution between the different periods of evaluation for each restorative material. In Figure 5, it is possible to observe the data trend in the function of time, demonstrating shrinkage after 5 min with expansion following until 10,000 cycles regardless of the restorative material. To elucidate the difference for each period of evaluation, Figure 6 shows the differences of means during two-sided confidence intervals with 95% coverage.

Table 4. Means of composites hygroscopic expansion at different aging cycles.

Material	Initial Volume	5 min	24 h	5000 Cycles	10,000 Cycles	15,000 Cycles	20,000 Cycles
Grandio	12.6924	12.4753	12.3366	12.9196	12.9712	12.9028	12.8062
Natural Look	12.8977	12.4655	12.4124	12.7651	12.6028	12.5833	12.5041
4Season	12.7869	12.4708	12.2934	13.0604	12.7115	12.7859	12.6772
EsthetX-HD	12.8141	12.4543	12.4198	13.0564	12.8844	12.9077	12.7392
Amaris	12.7433	12.4765	12.4549	13.0499	12.8212	12.8880	12.9252
Opallis	12.8696	12.4743	12.4426	13.0631	12.8871	12.9100	12.8878
Vit-l-lescence	12.9021	12.4864	12.3421	13.0600	12.8859	12.9371	12.8669
Filtek Z350	12.7648	12.4833	12.4285	13.1339	12.9876	12.9673	12.9285
P90	12.6060	12.4867	12.4735	13.1121	12.9719	12.9658	12.9592
Amelogen	12.8671	12.4823	12.4724	13.0355	12.9250	13.0264	12.9208
Venus	12.8718	12.5365	12.5253	13.1018	12.9525	12.9466	12.8691
Charisma	12.8208	12.4765	12.4533	13.1031	12.7304	13.0762	12.9795
Z250	12.8123	12.5367	12.4848	13.1532	13.0281	13.0199	12.9772

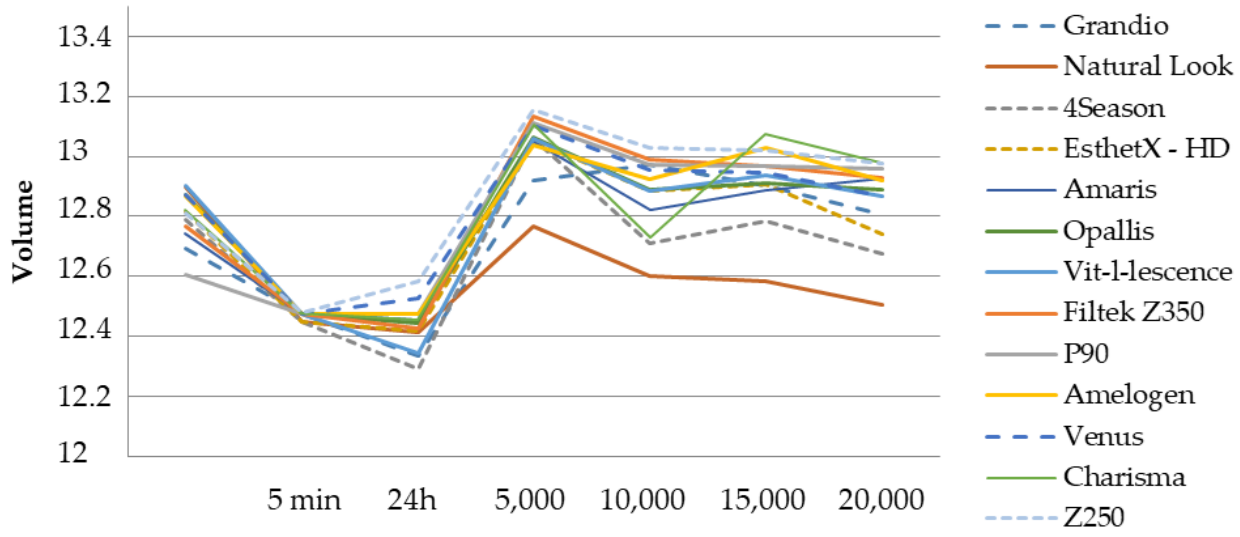

Figure 5. Resin composite hygroscopic expansion trend in function of the aging process progression (5 min, 24 h, 5000 to 20,000 thermal cycles.

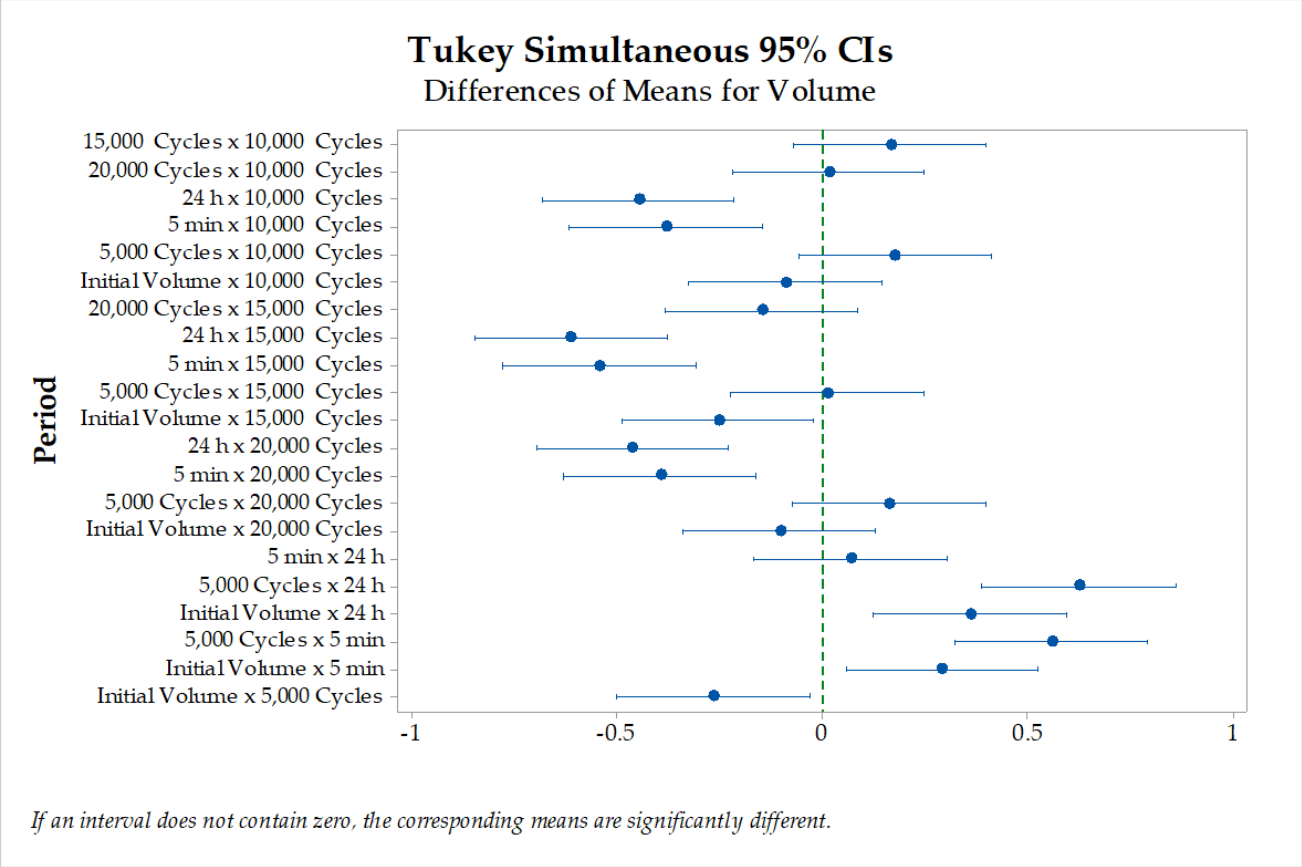

Figure 6. Tukey (95%) comparison for the difference of volume between the groups according to the different period of evaluation.

After normality check, the one-way ANOVA was performed considering Material as a factor for the evaluation of the elastic modulus, Poisson ratio, and degree of conversion data sets. The ANOVA test for the elastic modulus (GPa) presented F-value = 5.61 and p-value < 0.001 (Supplementary material: Table S3), while the for Poisson ratio presented F-value = 3.47 and p-value < 0.001 (Supplementary material: Table S4). For degree of conversion, the F-value was 33.19 and the p-value <0.001 (Supplementary material: Table S5). Therefore, there was a significant difference between materials for all three properties.

Table 5 summarizes the mean and standard deviation for elastic modulus measurement according to the different materials. The values ranged from 22.15 to 10.06 GPa. The major differences were observed between Grandio (22.15 ± 2.68 GPa) and Vit-L-Escence (16.24 ± 3.8 GPa) in comparison with 4 Seasons (10.06 ± 1.37 GPa).

Table 5. Mean and standard deviation for the elastic modulus (GPa) measurement according to the factor resin composite material. Same Capital Letter(s) means no statistical difference among groups ($\alpha = 0.05$).

Material	Mean ± Stand. Dev.	Grouping		
Grandio	22.15 ± 2.68	A		
Vit-L-Escence	16.24 ± 3.8	A	B	
Natural look	16.01 ± 1.34		B	C
Opallis	15.68 ± 1.5		B	C
Amaris	15.04 ± 0.93		B	C

Table 5. *Cont.*

Material	Mean ± Stand. Dev.	Grouping	
Charisma	13.77 ± 2.02	B	C
Z350	13.61 ± 0.27	B	C
Venus	13.33 ± 0.86	B	C
Z250	12.76 ± 0.83	B	C
EsthetX	12.75 ± 1.25	B	C
Amelogen	12.35 ± 1.05	B	C
P90	12.12 ± 0.58	B	C
4 Seasons	10.06 ± 1.37		C

For the Poisson ratio (Table 6) the values ranged from 0.54 until 0.22 (dimensionless). The major differences were observed between Grandio (0.54 ± 0.08) in comparison with 4 Seasons (0.31 ± 0.13), Z250 (0.30 ± 0.06), P90 (0.29 ± 0.11) and Amaris (0.22 ± 0.05).

Table 6. Mean and standard deviation for the Poisson ratio measurement according to the factor resin composite material. Same Capital Letter(s) means no statistical difference among groups ($\alpha = 0.05$).

Material	Mean ± Stand. Dev.	Grouping		
Grandio	0.54 ± 0.08	A		
Z350	0.47 ± 0.20	A	B	
Amelogen	0.41 ± 0.13	A	B	C
Vit-L-Escence	0.40 ± 0.12	A	B	C
Charisma	0.38 ± 0.13	A	B	C
Natural look	0.35 ± 0.10	A	B	C
Venus	0.35 ± 0.14	A	B	C
EsthetX	0.34 ± 0.10	A	B	C
Opallis	0.33 ± 0.14	A	B	C
4 Seasons	0.31 ± 0.13		B	C
Z250	0.30 ± 0.06		B	C
P90	0.29 ± 0.11		B	C
Amaris	0.22 ± 0.05			C

For the degree of conversion (Table 7), all evaluated materials showed more than 60% of conversion. The values ranged from 83.01 until 60.01 (%).

Table 7. Mean and standard deviation for the degree of conversion measurement according to the factor resin composite material. Same Capital Letter(s) means no statistical difference among groups ($\alpha = 0.05$).

Material	Mean ± Stand. Dev.	Grouping					
4 Seasons	83.01 ± 5.04	A					
Z350	78.63 ± 3.06	A	B				
P90	78.07 ± 4.41	A	B				
Z250	76.97 ± 2.82		B				
Amaris	70.92 ± 2.14			C			
Amelogen	69.36 ± 3.97			C	D		
Charisma	68.96 ± 3.28			C	D	E	
Natural look	68.63 ± 3.46			C	D	E	F
Opallis	64.62 ± 1.04				D	E	F
Grandio	63.60 ± 3.66				D	E	F
Venus	63.21 ± 1.92					E	F
Vit-L-Escence	62.93 ± 3.40						F
EsthetX	60.76 ± 1.84						

4. Discussion

The methodology applied for measuring the volumetric shrinkage by video-imaging the specimens was initially idealized for a simple verification of the shrinkage stress [33] as it was intended for a static platform. Regarding the immediate volumetric polymerization shrinkage, Filtek and Grandio presented the lowest mean value. After 24 h, the volumetric shrinkage of Grandio continued increasing, from 1.7% to 2.64% while Filtek increased just from 1.03% to 1.06%. Natural Look and 4 Seasons presented the highest values after 24 h, reaching 3.76% and 3.86%, respectively, an expected result for the Natural Look as it has lower viscosity.

From these results, it is possible to predict the need for a comparison between the groups just aged in hot water to isolate the effect of the temperature and the humidity separately, as these materials has been extensively used in dentistry for dental filling or cementation. The longevity of these materials will then depend upon a better combination of the aesthetic and mechanical properties as well as excellent techniques. Many materials used in the oral cavity have interactions with the wet environment and exposure to different temperature variations. The efficacy of adhesives and restorative materials is evaluated by exposing them to extreme temperature challenges, justifying the use of thermocycling as aging method. For the resin-based materials, this exposure promotes water diffusion through the organic matrix, resulting in hygroscopic expansion and chemical degradation [38,39]. This behavior can be noted as a hygroscopic expansion for all evaluated materials in the present study.

Previous studies have already verified that the water sorption can cause dimensional and weight alterations in the material after polymerization [40–42]. Some authors [40], showed a positive correlation between the absorbed water mass and the volume alteration. Water sorption promotes significant effects in the structure, physical properties, and dimensional alterations of composite materials with different organic matrix [43]. A previous method was described to measure the hygroscopic expansion of dental composites with time [44]. The method consists of using a laser microscope to make the volume measurements on rotating composite samples while the computer processes the data statistically, which motivated the authors from the present study to use the AcuvolTM equipment with the same purpose.

The effect of the humidity exposition resulting in an increase of the dental composite volume can be demonstrated in many ways, such as measurements of the length [45] and relaxation of the shrinkage stresses developed by the polymerization [46]. The ability of the water molecule to diffuse through the organic matrix of the composite determines the hydrophobicity of the material, while the elasticity and bond strength will determine the dimensions of the material. The elastic limit of the polymer and co-polymers chemical bonding determines the maximum amount that the material will expand. Finally, dimensional alteration after the first aging cycling can happen due to the hydrolytic degradation of the bonding into the polymer formed. The majority of the composites studied have hydrophobic nature coming from the monomers used on its composition.

For dental composites, in order to effectively reduce the polymerization stress during resin placement, a material with low post-gel shrinkage must be associated to a relatively low elastic modulus [2]. This can be justified because, in summary, the higher the elastic modulus of the restorative material, the smaller the deformation of dental structures under the same stress [36]. However, a reduction in the dental composite elastic modulus could lead to low hardness and low wear strength. Therefore, eventually generating higher marginal misfit, post-operative sensitivity or dental fracture, compromising the longevity of the dental treatment [9]. To compensate this, an intermediate elastic modulus material should be preferable and the multilayer technique applied as a practical and effective approach to lower the shrinkage stresses by adding a base layer under the restorative material [21]. Biomaterials that possess adequate compressive and tensile strength and relatively low elastic modulus could act as a cushion layer to the shrinkage stress transmitted to the tooth tissues [21]. However, in adhesive restorations, the mechanical behavior

under compressive loading and shrinkage stress can be associated with several factors other than the material, including the enamel and dentine volumes lost [4]. In this study, the highest Elastic modulus mean value was observed for Grandio (22.15 ± 2.68 GPa) and the lowest for 4 Seasons (10.06 ± 1.37 GPa), as observed in Table 5. Poisson ratio is normally between 0 and 1 and refers to the ratio between expansion and contraction under tensile or compressive loads. The results showed accordance with the literature through mean values ranging from 0.54 (Grandio) until 0.22 (Amaris) (Table 6).

Few studies are focused on the thermocycling effect in water sorption, solubility and hygroscopic expansion of composites. Previous authors [39] evaluated the water sorption and solubility of resin-based materials, following a thermocycle protocol initially purposed by Gale and Darvell in 1999 [47] after an in vivo evaluation. In the present study, different materials were not different statistically. All composites had a great reduction in volume just after the polymerization, reducing slowly until 24 h. After the water immersion, the volume trend showed an inverse progression that stabilized after 10,000 cycles. The reason and the amount of polymer hygroscopic expansion depends on many factors, such as the type of matrix, filler, bonding between filler and organic matrix, and the volumetric ratio between the inorganic and organic matrix [40,42,48]. Another study pointed to a great expansion occurring at the first week and a gradual increase, however slow, during the first six months [41].

The conversion degree of monomers to polymers in dental resins can be evaluated using hardness tests or FT-Raman spectroscopy [37]. The degree of conversion is one of the critical parameters that may influence the physical properties of resin composite materials and thus the expected clinical behavior of restorations made of polymeric materials [37]. Previous researchers that have used different indirect methods to evaluate restorative resins' DC reported values ranging from 50% to 80% [49]. These values are in agreement with the results calculated (Table 7) in the present study (more than 60% for all materials). However, the degree of conversion as an isolated factor does not allow the proper ranking of different materials in terms of functional longevity, since it can be affected by the light-source, materials stiffness, and volume of resin.

It is already known that high temperature promotes a significant increase in the resin-based material degradation [50,51]. In this way, the present study was based on maximum and minimum temperatures, simulating the extreme conditions that would not surpass this limit, to consider the clinical values that could still be present in the majority of the researches evaluating the effect of aging on bonded interfaces. Other authors observed an increase in water sorption in composites when increasing the number of cycles, regardless of the energy font and the material, which was also observed in the present study [49]. The sorption and diffusion of fluids through the polymer are affected by the liquid density used during the cycles which are also influenced by the room temperature [44].

Although the statistical analysis does not show any differences among the evaluated materials used, Natural Look composite presented the lowest final volume when compared to Z250 and Charisma. This could have happened because UDMA polymer absorb less water than BisGMA, due to its higher crosslinking ability [51–53]. Another factor that can explain these small differences could be the amount of filler in each material, as there is an inverse correlation with the degree of hygroscopic expansion and water sorption. As the filler volume increases, there is a decrease in the water sorption and consequently the hygroscopic expansion [42]. A study idealized the influence of the filler/matrix interface [53], where a poor bonding would provide a way of facilitating the water diffusion, then a material with high filler volume would accommodate the water volume in this region.

The silane treatment of the filler gives a bonding resin-to-filler and has been shown to enhance the mechanical stability of the filler–matrix interface, increasing the strength and hardness of composite resins [54]. The inclusion of an effective coupling agent in the composite significantly reduces the rate of diffusion along the grain boundary and leaves only normal diffusion confined to the matrix alone [50]. Another possible explanation for the higher values seen for the volume changes of some composites could be the weak

bonding between the cement particles and the resin matrix. The filler treatment and presence of interspacing caused by a poor silanization process can affect the surface energy of the fillers, as any of those are considered defects in the material and concentrate stress. The surface energy of the glass particles under the water or saliva (whose proteins will be absorbed) is lower than when in air. In this wet condition, the initiation of the crack/flaw is then facilitated, requiring little effort, such as stresses generated after polymerization shrinkage. Consequently, the adhesion of the particles to the matrix can be destroyed by hydrolysis [52–57]. If the material is inhomogeneous and anisotropic, as almost all dental materials are, several sizes of defects can be present [58]. This potential deterioration of the glass is one of the reasons why it is so important to form an organic layer of silane molecules on the surface of the filler to protect it from the environment [56–58]. No matter what the application or the chemistry of the polymer present in the resin cements, the properties investigated in this study show that future studies are needed considering composite integrity. In addition, further studies should be carried out to investigate the effect of different monomer ratios and how they can affect the volumetric shrinkage of the current dental materials.

5. Conclusions

Within the limitations of this study, it was concluded that:

- The polymerization shrinkage is dependent upon the type of composite and can be different between materials with similar Elastic moduli.
- The termocycling aging has a significant influence on the water sorption in the evaluated materials.

Supplementary Materials: The following are available online at https://www.mdpi.com/article/10.3390/jcs5120322/s1, Table S1: Two-Way ANOVA for the volumetric shrinkage according to the resin composite materials and post-polymerization time, Table S2: Two-Way ANOVA for the hygroscopic expansion according to the resin composite materials and Period of evaluation, Table S3: One-Way ANOVA for the elastic modulus according to the resin composite material, Table S4: One-Way ANOVA for the Poisson ratio according to the resin composite material, Table S5: One-Way ANOVA for the degree of conversion according to the resin composite material.

Author Contributions: Conceptualization, A.L.S.B.; methodology, A.L.S.B., A.M.d.O.D.P., and J.P.M.T.; software, A.L.S.B. and J.P.M.T.; validation, A.L.S.B., S.E.M., and R.C.d.M.; formal analysis, A.L.S.B., A.M.d.O.D.P., S.E.M., and J.P.M.T.; investigation, A.L.S.B., R.C.d.M., and J.P.M.T.; resources, A.L.S.B. and J.P.M.T.; data curation, A.L.S.B., A.M.d.O.D.P., and J.P.M.T.; writing—original draft preparation, A.L.S.B., S.E.M., and R.C.d.M.; writing—review and editing, A.M.d.O.D.P. and J.P.M.T.; visualization, A.M.d.O.D.P. and J.P.M.T.; supervision, A.L.S.B. and J.P.M.T.; project administration, A.L.S.B.; funding acquisition, A.L.S.B. and J.P.M.T. All authors have read and agreed to the published version of the manuscript.

Funding: São Paulo Research Foundation (FAPESP) supported this study with the grant nº 2010/51749-3 and National Counsel of Technological and Scientific Development (CNPq) with the grant nº 201980/2011-8.

Data Availability Statement: Data available on request of the first author.

Acknowledgments: The authors would like to thank São Paulo Research Foundation (FAPESP) nº 2010/51749-3 and National Counsel of Technological and Scientific Development (CNPq) nº 201980/2011-8.

Conflicts of Interest: The authors declare no conflict of interest.

References

1. Piconi, C.; Sprio, S. Oxide bioceramic composites in orthopedics and dentistry. *J. Compos. Sci.* **2021**, *5*, 206. [CrossRef]
2. Boaro, L.C.C.; Gonçalves, F.; Guimarães, T.C.; Ferracane, J.L.; Versluis, A.; Braga, R.R. Polymerization stress, shrinkage and elastic modulus of current low-shrinkage restorative composites. *Dent. Mater.* **2010**, *26*, 1144–1150. [CrossRef] [PubMed]

3. Irie, M.; Maruo, Y.; Nishigawa, G.; Matsumoto, T. Flexural Property of a Composite Biomaterial in Three Applications. *J. Compos. Sci.* **2021**, *5*, 282. [CrossRef]
4. Matuda, A.G.N.; Silveira, M.P.M.; de Andrade, G.S.; de Piva, A.M.O.D.; Tribst, J.P.M.; Borges, A.L.S.; Testarelli, L.; Mosca, G.; Ausiello, P. Computer aided design modelling and finite element analysis of premolar proximal cavities restored with resin composites. *Materials* **2021**, *14*, 2366. [CrossRef]
5. Francesco, P.; Gabriele, C.; Fiorillo, L.; Giuseppe, M.; Antonella, S.; Giancarlo, B.; Mirta, P.; Mendes Tribst, J.P.; Lo Giudice, R. The use of bulk fill resin-based composite in the sealing of cavity with margins in radicular cementum. *Eur. J. Dent.* **2021**. [CrossRef] [PubMed]
6. Ajaj, R.A.; Farsi, N.J.; Alzain, L.; Nuwaylati, N.; Ghurab, R.; Nassar, H.M. Dental bulk-fill resin composites polymerization efficiency: A systematic review and meta-analysis. *J. Compos. Sci.* **2021**, *5*, 149. [CrossRef]
7. Gordan, V.V.; Garvan, C.W.; Blaser, P.K.; Mondragon, E.; Mjor, I.A. A long-term evaluation of alternative treatments to replacement of resin-based composite restorations: Results of a seven-year study. *J. Am. Dent. Assoc.* **2009**, *140*, 1476–1484. [CrossRef]
8. Lundin, S.A.; Rasmusson, C.G. Clinical evaluation of a resin composite and bonding agent in Class I and II restorations: 2-year results. *Quintessence Int.* **2004**, *35*, 758–762.
9. Davidson, C.L.; de Gee, A.J.; Feilzer, A. The competition between the composite-dentin bond strength and the polymerization contraction stress. *J. Dent. Res.* **1984**, *63*, 1396–1399. [CrossRef]
10. Torres, C.R.; Jurema, A.L.; Souza, M.Y.; Di Nicoló, R.; Borges, A.B. Bulk-fill versus layering pure ormocer posterior restorations: A randomized split-mouth clinical trial. *Am. J. Dent.* **2021**, *34*, 143–149. [PubMed]
11. Serin, B.A.; Yazicioglu, I.; Deveci, C.; Dogan, M.C. Clinical evaluation of a self-adhering flowable composite as occlusal restorative material in primary molars: One-year results. *Eur. Oral Res.* **2019**, *53*, 119–124. [CrossRef]
12. Shahmoradi, M.; Wan, B.; Zhang, Z.; Swain, M.; Li, Q. Mechanical failure of posterior teeth due to caries and occlusal wear—A modelling study. *J. Mech. Behav. Biomed. Mater.* **2021**, *125*, 104942. [CrossRef] [PubMed]
13. Costa, A.R.; Naves, L.Z.; Garcia-Godoy, F.; Tsuzuki, F.M.; Correr, A.B.; Correr-Sobrinho, L.; Puppin-Rontani, R.M. CHX stabilizes the resin/demineralized dentin interface. *Braz. Dent. J.* **2021**, *32*, 106–115. [CrossRef]
14. Correia, A.M.O.; Andrade, M.R.; Tribst, J.P.M.; Borges, A.L.S.; Caneppele, T.M.F. Influence of bulk-fill restoration on polymerization shrinkage stress and marginal gap formation in Class V restorations. *Oper. Dent.* **2020**, *45*, E207–E216. [CrossRef] [PubMed]
15. Dávila-Sánchez, A.; Gutierrez, M.F.; Bermudez, J.P.; Méndez-Bauer, L.; Pulido, C.; Kiratzc, F.; Alegria-Acevedo, L.F.; Farago, P.V.; Loguercio, A.D.; Sauro, S.; et al. Effects of dentine pretreatment solutions containing flavonoids on the resin polymer-dentine interface created using a modern universal adhesive. *Polymers* **2021**, *13*, 1145. [CrossRef] [PubMed]
16. Behl, S.; Rajan, G.; Farrar, P.; Prentice, L.; Prusty, B.G. Evaluation of depth-wise post-gel polymerisation shrinkage behaviour of flowable dental composites. *J. Mech. Behav. Biomed. Mater.* **2021**, *124*, 104860. [CrossRef]
17. D'Alpino, P.H.; Bechtold, J.; dos Santos, P.J.; Alonso, R.C.; Di Hipolito, V.; Silikas, N.; Rodrigues, F.P. Methacrylate- and silorane-based composite restorations: Hardness, depth of cure and interfacial gap formation as a function of the energy dose. *Dent. Mater.* **2011**, *27*, 1162–1169. [CrossRef]
18. Tauböck, T.T.; Feilzer, A.J.; Buchalla, W.; Kleverlaan, C.J.; Krejci, I.; Attin, T. Effect of modulated photo-activation on polymerization shrinkage behavior of dental restorative resin composites. *Eur. J. Oral Sci.* **2014**, *122*, 293–302. [CrossRef]
19. Gregor, L.; Dorien, L.; Bortolotto, T.; Feilzer, A.J.; Krejci, I. Marginal integrity of low-shrinking versus methacrylate-based composite: Effect of different one-step self-etch adhesives. *Odontology* **2017**, *105*, 291–299. [CrossRef]
20. Rodrigues, F.P.; Silikas, N.; Watts, D.C.; Ballester, R.Y. Finite element analysis of bonded model Class I 'restorations' after shrinkage. *Dent. Mater.* **2012**, *28*, 123–132. [CrossRef]
21. Sun, T.; Shao, B.; Liu, Z. Effects of the lining material, thickness and coverage on residual stress of class II molar restorations by multilayer technique. *Comput. Methods Progr. Biomed.* **2021**, *202*, 105995. [CrossRef]
22. Feilzer, A.J.; De Gee, A.J.; Davidson, C.L. Setting stress in composite resin in relation to configuration of the restoration. *J. Dent. Res.* **1987**, *66*, 1636–1639. [CrossRef] [PubMed]
23. Aregawi, W.A.; Fok, A.S.L. Shrinkage stress and cuspal deflection in MOD restorations: Analytical solutions and design guidelines. *Dent. Mater.* **2021**, *37*, 783–795. [CrossRef] [PubMed]
24. Versluis, A.; Tantbirojn, D.; Douglas, W.H. Do dental composites always shrink toward the light? *J. Dent. Res.* **1998**, *77*, 1435–1445. [CrossRef]
25. Goncalves, F.; Boaro, L.C.; Ferracane, J.L.; Braga, R.R. A comparative evaluation of polymerization stress data obtained with four different mechanical testing systems. *Dent. Mater.* **2012**, *28*, 680–686. [CrossRef]
26. Ghavami-Lahiji, M.; Hooshmand, T. Analytical methods for the measurement of polymerization kinetics and stresses of dental resin-based composites: A review. *Dent. Res. J.* **2017**, *14*, 225.
27. Enochs, T.; Hill, A.E.; Worley, C.E.; Veríssimo, C.; Tantbirojn, D.; Versluis, A. Cuspal flexure of composite-restored typodont teeth and correlation with polymerization shrinkage values. *Dent. Mater.* **2018**, *34*, 152–160. [CrossRef] [PubMed]
28. Labella, R.; Lambrechts, P.; Van Meerbeek, B.; Vanherle, G. Polymerization shrinkage and elasticity of flowable composites and filled adhesives. *Dent. Mater.* **1999**, *15*, 128–137. [CrossRef]
29. Dauvillier, B.S.; Aarnts, M.P.; Feilzer, A.J. Developments in shrinkage control of adhesive restoratives. *J. Esthet. Dent.* **2000**, *12*, 291–299. [CrossRef] [PubMed]

30. Dauvillier, B.S.; Feilzer, A.J.; de Gee, A.J.; Davidson, C.L. Visco-elastic parameters of dental restorative materials during setting. *J. Dent. Res.* **2000**, *79*, 818–823. [CrossRef]
31. De Gee, A.F.; Feilzer, A.J.; Davidson, C.L. True linear polymerization shrinkage of unfilled resins and composites determined with a linometer. *Dent. Mater.* **1993**, *9*, 11–14. [CrossRef]
32. Mitrović, A.; Antonović, D.; Tanasić, I.; Mitrović, N.; Bakić, G.; Popović, D.; Milošević, M. 3D digital image correlation analysis of the shrinkage strain in four dual cure composite cements. *Biomed Res. Int.* **2019**, *2019*, 2041348. [CrossRef] [PubMed]
33. Barcellos, D.C.; Fonseca, B.M.; Pucci, C.R.; das Cavalcanti, B.N.; Persici, E.D.S.; de Gonçalves, S.E.P. Zn-doped etch-and-rinse model dentin adhesives: Dentin bond integrity, biocompatibility, and properties. *Dent. Mater.* **2016**, *32*, 940–950. [CrossRef]
34. Correa Netto, L.R.; Borges, A.L.S.; Guimarães, H.B.; de Almeida, E.R.N.; Poskus, L.T.; da Silva, E.M. Marginal integrity of restorations produced with a model composite based on polyhedral oligomeric silsesquioxane (POSS). *J. Appl. Oral Sci.* **2015**, *23*, 450–458. [CrossRef]
35. Otani, L.B.; Pereira, A.H.A.; Melo, J.D.D.; Amico, S.C. *Elastic Moduli Characterization of Composites Using the Impulse Excitation*. Technical-Scientific Informative ATCP Physical Engineering: White Paper. 2014. Available online: https://www.google.com/url?sa=t&rct=j&q=&esrc=s&source=web&cd=&cad=rja&uact=8&ved=2ahUKEwjmudHRrtT0AhVOM-wKHb7OCAUQFnoECAoQAQ&url=http%3A%2F%2Fsonelastic.com%2Fimages%2Fdownloads%2FITC-06-IET-MOE-Composites-v1.4.pdf&usg=AOvVaw03MzFa2VG4wTulMT7EhhRp (accessed on 10 December 2021).
36. Meirelles, L.C.F.; Pierre, F.Z.; Tribst, J.P.M.; Pagani, C.; Bresciani, E.; Borges, A.L.S. Influence of preparation design, restorative material and load direction on the stress distribution of ceramic veneer in upper central incisor. *Braz. Dent. Sci.* **2021**, *24*. [CrossRef]
37. Souza, R.O.A.; Ozcan, M.; Mesquita, A.M.M.; De Melo, R.M.; Galhano, G.A.P.; Bottino, M.A.; Pavanelli, C.A. Effect of different polymerization devices on the degree of conversion and the physical properties of an indirect resin composite. *Acta Odontol. Latinoam.* **2010**, *23*, 129–135. [PubMed]
38. Walter, R.; Swift, E.J., Jr.; Sheikh, H.; Ferracane, J.L. Effects of temperature on composite resin shrinkage. *Quintessence Int.* **2009**, *40*, 843–847. [PubMed]
39. Szczesio-Wlodarczyk, A.; Sokolowski, J.; Kleczewska, J.; Bociong, K. Ageing of dental composites based on methacrylate resins—A critical review of the causes and method of assessment. *Polymers* **2020**, *12*, 882. [CrossRef] [PubMed]
40. Colombo, M.; Gallo, S.; Chiesa, M.; Poggio, C.; Scribante, A.; Zampetti, P.; Pietrocola, G. In vitro weight loss of dental composite resins and glass-ionomer cements exposed to A challenge simulating the oral intake of acidic drinks and foods. *J. Compos. Sci.* **2021**, *5*, 298. [CrossRef]
41. Yadav, R.; Kumar, M. Dental restorative composite materials: A review. *J. Oral Biosci.* **2019**, *61*, 78–83. [CrossRef] [PubMed]
42. Maia, K.M.F.V.; Rodrigues, F.V.; Damasceno, J.E.; Ramos, R.V.D.C.; Martins, V.L.; Lima, M.J.P.; Cavalcanti, A.N. Water sorption and solubility of a nanofilled composite resin protected against erosive challenges. *Braz. Dent. Sci.* **2019**, *22*, 46–54. [CrossRef]
43. Martin, N.; Jedynakiewicz, N.M.; Fisher, A.C. Hygroscopic expansion and solubility of composite restoratives. *Dent. Mater.* **2003**, *19*, 77–86. [CrossRef]
44. Martin, N.; Jedynakiewicz, N. Measurement of water sorption in dental composites. *Biomaterials* **1998**, *19*, 77–83. [CrossRef]
45. Chutinan, S.; Platt, J.A.; Cochran, M.A.; Moore, B.K. Volumetric dimensional change of six direct core materials. *Dent. Mater.* **2004**, *20*, 345–351. [CrossRef]
46. Feilzer, A.J.; de Gee, A.J.; Davidson, C.L. Relaxation of polymerization contraction shear stress by hygroscopic expansion. *J. Dent. Res.* **1990**, *69*, 36–39. [CrossRef]
47. Gale, M.S.; Darvell, B.W. Thermal cycling procedures for laboratory testing of dental restorations. *J. Dent.* **1999**, *27*, 89–99. [CrossRef]
48. Wei, Y.-J.; Chen, Y.-Y.; Jiang, Q.-S. Long-term hygroscopic dimensional changes of core buildup materials in deionized water and artificial saliva. *Dent. Mater. J.* **2021**, *40*, 143–149. [CrossRef] [PubMed]
49. Catalbas, B.; Uysal, T.; Nur, M.; Demir, A.; Gunduz, B. Effects of thermocycling on the degree of cure of two lingual retainer composites. *Dent. Mater. J.* **2010**, *29*, 41–46. [CrossRef] [PubMed]
50. Mair, L.H. Effect of surface conditioning on the abrasion rate of dental composites. *J. Dent.* **1991**, *19*, 100–106. [CrossRef]
51. Montes, G.G.; Draughn, R.A. In vitro surface degradation of composites by water and thermal cycling. *Dent. Mater.* **1986**, *2*, 193–197. [CrossRef]
52. Kaneko, O.; Asakura, M.; Hayashi, T.; Kato, D.; Ban, S.; Kawai, T.; Murakami, H. Effect of degradation of filler elements on flexural strength for dental CAD/CAM resin composite materials in water. *J. Prosthodont. Res.* **2021**, *65*, 509–514. [CrossRef] [PubMed]
53. Kalachandra, S. Influence of fillers on the water sorption of composites. *Dent. Mater.* **1989**, *5*, 283–288. [CrossRef]
54. Ferracane, J.L. Hygroscopic and hydrolytic effects in dental polymer networks. *Dent. Mater.* **2006**, *22*, 211–222. [CrossRef] [PubMed]
55. Apicella, A.; Di Palma, L.; Aversa, R.; Ausiello, P. DSC kinetic characterization of dental composites using different light sources. *J. Adv. Mater.* **2002**, *34*, 22–25.
56. Han, L.; Okamoto, A.; Fukushima, M.; Okiji, T. Evaluation of physical properties and surface degradation of self-adhesive resin cements. *Dent. Mater. J.* **2007**, *26*, 906–914. [CrossRef] [PubMed]

57. Tseng, C.-C.; Lin, P.-Y.; Kirankumar, R.; Chuang, Z.-W.; Wu, I.-H.; Hsieh, S. Surface degradation effects of carbonated soft drink on a resin based dental compound. *Heliyon* **2021**, *7*, e06400. [CrossRef] [PubMed]
58. Borges, A.L.S.; Tribst, J.P.M.; Dal Piva, A.M.O.; Souza, A.C.O. In vitro evaluation of multi-walled carbon nanotube reinforced nanofibers composites for dental application. *Int. J. Polym. Mater.* **2020**, *69*, 1015–1022. [CrossRef]